Desalination and Water Treatment
www.deswater.com
doi: 10.1080/19443994.2012.749368

51 (2013) 2726–2739
March

Taylor & Francis
Taylor & Francis Group

Modeling of adsorption isotherms and kinetics of Remazol Red RB adsorption from aqueous solution by modified clay

S. Karaca[a,*], A. Gürses[b], Ö. Açışlı[a], A. Hassani[a], M. Kıranşan[a], K. Yıkılmaz[a]

[a]*Faculty of Science, Department of Chemistry, Atatürk University, 25240 Erzurum, Turkey*
Tel. +90 442 231 4435; Fax: +90 442 236 0948; email: skaraca@atauni.edu.tr
[b]*K.K. Education Faculty, Department of Chemistry, Atatürk University, 25240 Erzurum, Turkey*

Received 23 March 2012; Accepted 30 July 2012

ABSTRACT

The adsorption of an anionic dye Remazol Red RB, from aqueous solution on modified clay was investigated at 298, 313, and 333 K. Different parameters that influence the adsorption process such as contact time, initial dye concentration, solution pH, and temperature were systematically studied. Adsorption capacity increased with increasing of temperature, initial dye concentration, and pH. The value of zeta potential decreased with increasing of pH. Experimental adsorption data were modeled by different equilibrium isotherms such as Langmuir, Freundlich, Temkin, Dubinin–Radushkevich (D–R), Brunauer-Emmett-Teller (BET), Halsey, Harkins–Jura, Smith, and Henderson isotherms. The adsorption process followed the Langmuir isotherm model with high coefficients of correlation ($R^2 > 0.99$) at different temperatures. The pseudo-second-order kinetic model fitted well in correlation to the experimental results. Activation energy of the adsorption process (E_a) was found to be 34.49 kJ mol^{-1} and 40.27 kJ mol^{-1} for initial dye concentrations of 75 and 150 mg/L, respectively—by using the Arrhenius equation, indicating the strong electrostatic interactions between the adsorbent and dye. Thermodynamic parameters suggest that the adsorption process is spontaneous and endothermic in nature.

Keywords: Adsorption isotherms; Adsorption; Remazol Red RB; Modified clay; Kinetic

1. Introduction

The thermodynamic characterization of a solid–liquid interface is very important for a wide range of problems in pure and applied surface science. This is also of great interest in the case of the textile industry because of their practical applications. In fact, dye adsorption depends to a large extent on the surface free-energy interactions involved. Although such systems are usually complicated, an investigation of the adsorption kinetics and thermodynamic properties provide better information concerning the mechanism of adsorption [1]. The rate at which the dye molecules are transferred to the adsorbent may be influenced by the transport of dye through the bulk solution to the surface of the adsorbent, the possible adsorption of dye molecules onto this surface, and the diffusion of the dye from the surface to the interior of the adsorbent [2].

Azo dyes are the main chemical class of dyes with the greatest variety of colors, and therefore, they have been extensively used in the industrial fields. These dyes are characterized by one or more azo linkages (R_1–N=N–R_2) and by aromatic structures. The biological effects of azo dyes after biotransformation have

*Corresponding author.

been shown to be toxic; and in some cases, these compounds are carcinogenic and mutagenic [3]. Therefore, the treatment of effluents containing such dyes is of prime importance due to their harmful impacts on receiving waters. The disposal of dye wastewater with proper treatment is a big challenge. This is mainly because synthetic dyes used in industries are designed to resist fading upon exposure to sweat, heat, light, water, many chemicals including oxidizing agents, and microbial attacks [4,5]. The traditional methods for color removal include photocatalytic degradation, sonochemical degradation, micellar enhanced ultrafiltration, cation exchange membranes, electrochemical degradation, integrated chemical–biological degradation, integrated iron(III) photoassisted-biological treatment, solar photo-Fenton and biological processes, and Fenton-biological treatment scheme [5]. However, all these methods have disadvantages like incomplete removal, high reagent and energy generation of toxic sludge or other waste products that require careful disposal, high capital and operating costs, labor intensive etc. In this light, adsorption has emerged as an efficient and cost-effective alternative to conventional contaminated-water treatment facilities. Adsorption is defined as a process wherein a material is concentrated at a solid surface from its liquid or gaseous surroundings [6]. Adsorption separation in environmental engineering is now an esthetic attention and consideration among the countries, owing to its low initial cost, simplicity of design, ease of operation, insensitivity to toxic substances, and complete removal of pollutants even from their dilute solutions [4]. Adsorption also does not result in the formation of harmful substances.

The adsorption characteristics of dyes on various adsorbents have previously been extensively investigated for many purposes of separation and purification. Although activated carbon remains the most widely used adsorbent, its relatively high cost restricts its use somewhat. However, in addition to cost, adsorptive properties and availability are also key criteria when it comes to choosing an adsorbent for pollutant removal, thereby encouraging research into materials that are both efficient and cheap. Indeed, several authors have reported the use of adsorbents such as eggshells [7], chitosan [8], peat [9], wood [10], waste [11], red mud [12], fly ash [12,13], and clays [14]. Clays have a high adsorption capacity due to their lamellar structure which provides increased specific surface areas [15] and possibility to adsorb ions and polar organic molecules on particle external site and in interlayer positions [16]. Adsorption and desorption of organic molecules in the clays are primarily controlled by surface properties of the clay and the chemical properties of the molecules [17]. Natural clay exhibits a negative charge of structure which allows it to adsorb positively charged dyes but induces a low adsorption capacity for anionic dyes. Thus, literature mostly reports on cationic dye adsorption by clay and very few studies have been devoted to anionic dye adsorption onto natural clay [18–21] or treated clay [22]. The present study is aimed to study a convenient and economic method for Remazol Red RB removal from water by adsorption on modified clay, to gain an understanding of the adsorption kinetics, to describe the rate and mechanism of adsorption, to determine the factors controlling the rate of adsorption, and to calculate the activation energy of the system. The adsorption models were applied to describe the equilibrium isotherms and the isotherm constants were also determined. In addition, the thermodynamic activation parameters, such as enthalpy, entropy, and the free energy were investigated to provide insights into the adsorption reactions and mechanisms.

2. Experimental

2.1. Chemicals

In this study, montmorillonite clay which has been modified with 35–45 wt.% dimethyl dialkyl (C_{14}–C_{18}) amine and has a zeta potential value of 74.5 mV (Sigma Aldrich cat. no. 682624) was used as adsorbent. The anionic dye used in the study is Remazol Red RB (C.I. Reactive Red 22 (RR 22), 14282), 2-(3-amino-4-methoxy phenyl sulfonyl) ethanol sulfate ester → 1-naphthyl-5-sulfonic acid (Fig. 1). It is widely used in dyeing cotton and was obtained from textile industry in the Marmara region of Turkey. All chemicals used in this study were purchased from Merck and were used without any further purification.

2.2. Adsorption experiments

Adsorption experiments were carried out in 100-mL glass-stoppered round-bottom flasks immersed in a thermostatic shaker bath. For this, 0.1 g of adsorbent sample was mixed with 100 mL of the aqueous

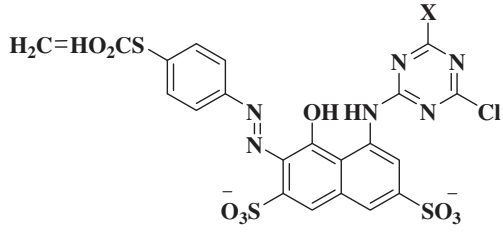

Fig. 1. Structure of Remazol Red RB (hypothesized).

solutions of the various initial concentrations (25, 50, 75, 100, 125, and 150 mg/L) of Remazol Red RB. The flasks with their contents were shaken for different adsorption times at the temperatures 298, 313, and 333 K and natural pH (pH = 6.0). The effect of pH was investigated at 298 K for 90 min. The initial pHs (1, 3, 5, 7, 9, and 10) of the solutions were adjusted with concentrated HCl and NaOH solution and measured by a WTW inoLab pH meter (WTW Inc., Weilheim, Germany). The pH meter was standardized with buffers before every measurement. In the experiments, the stirring speed was kept constant at 90 min^{-1}. At the end of the adsorption period, the supernatant was centrifuged for 5 min at 6,000 min^{-1}. The concentration of Remazol Red RB in the supernatant solution after and before adsorption was determined with a 1.0 cm light path quartz cell using Varian Cary 100 UV spectrophotometer at λ_{max} of 540 nm. It was found that the supernatant from the adsorbent samples did not exhibit any absorbance at this wavelength and also that the calibration curve was very reproducible and linear over the concentration range used in this work. The amount of Remazol Red RB adsorbed was calculated from the difference between the concentrations in the solution before and after adsorption. Blanks containing no Remazol Red RB were used for each series of experiments. The amount of Remazol Red RB adsorbed per gram of adsorbent was calculated using following equation:

$$q = (C_0 - C_e)V/w \quad (1)$$

where q is Remazol Red RB uptake (mg/g), C_0 is the initial concentration of Remazol Red RB(mg/L), C_e is the equilibrium concentration of Remazol Red RB (mg/L), V is the volume of solution (L), and w is the dry weight of the added adsorbent (g).

2.3. Zeta potential and conductivity measurements

Zeta potentials of solid particles in modified clay/water suspensions from the experiments at different initial pHs (1, 3, 5, 7, 9, and 10) were measured by using Zeta Meter 3.0+ (Zeta-Meter, Inc., Staunton, VA, USA) for a constant adsorption time, 90 min. The zeta potential values were corrected for temperature differences using the following equation:

$$\zeta_d \text{ (mV)} = C_T\zeta_0 \quad (2)$$

where ζ_d, C_T, and ζ_0 represent the corrected zeta potential value, correction factor related to temperature, and the measured zeta potential value, respectively. In addition, prior to each measurement, the zeta meter was calibrated using a Min-U-Sil standard solution. Min-U-Sil is a natural air-floated silica produced by crushing sandstone. Its average diameter is about 1.1 μm. A suspension of 100 mg/L of Min-U-Sil in a 100 mg/L sodium chloride solution is easy to prepare and gives reasonably consistent results. This suspension was allowed to stand for 1 h to reach equilibrium before use. The average zeta potential of the Min-U-Sil standard solution was between −50 mV and −42 mV with a standard deviation of 4–6 mV.

Conductivity measurements, by using a WTW LF 521 Karl Kolb conductometer (WTW Inc., Weilheim, Germany), were determined after adsorption under the same conditions as zeta potential measurements.

3. Results and discussion

3.1. Effect of initial adsorbate concentration on adsorption process

To determine proper Remazol Red RB adsorption and equilibrium time, initial concentrations of Remazol Red RB solutions were changed and time intervals were assessed until no adsorption of adsorbate on organo clay surface takes place. Figs. 2–4 show the extent of dye adsorption as a function of reaction time and initial dye concentration. Results show that dye adsorption reaches to equilibrium adsorption in 90 min. Based on these results, 90 min was taken as the equilibrium time in kinetic adsorption experiments. At this point, the amounts of dye being adsorbed onto modified clay sample were in a state of dynamic equilibrium, with the amount of dye desorbed from adsorbent.

Because initial dye concentration has important role for mass transfer between the aqueous and solid

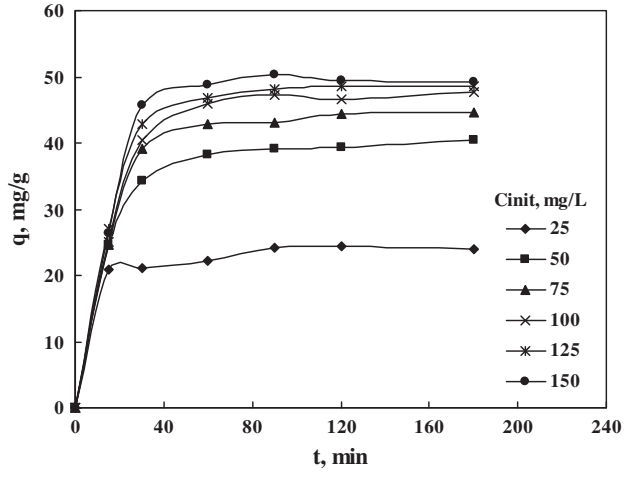

Fig. 2. The variation of the amount of adsorbed (q) with adsorption time at various initial dye concentrations for 298 K. Adsorbent amount 0.1 g, contact time 90 min, stirring speed 90 min^{-1}, and natural pH.

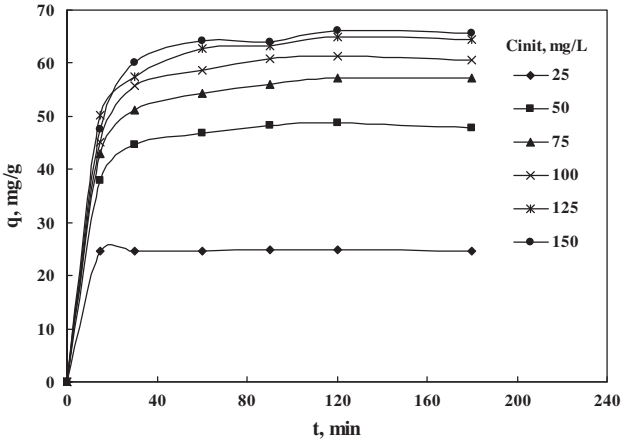

Fig. 3. The variation of the amount of adsorbed (q) with adsorption time at various initial dye concentrations for 313 K. Adsorbent amount 0.1 g, contact time 90 min, stirring speed 90 min^{-1}, and pH natural.

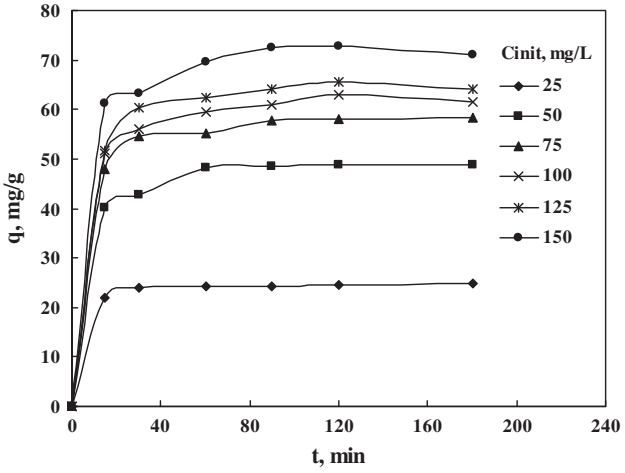

Fig. 4. The variation of the amount of adsorbed (q) with adsorption time at various initial dye concentrations for 333 K. Adsorbent amount 0.1 g, contact time 90 min, stirring speed 90 min^{-1}, and pH natural.

phase, the effect of initial dye concentration on the adsorbent was studied at 25, 50, 75, 100, 125, and 150 mg/L concentrations. It can be seen that the percentage removal of dye decreases with increase in initial dye concentration. At first, the adsorption rate may be higher because of an increase in the number of vacant sites initially available, resulting in an increased concentration gradient between the sorbate in the solution and that at the sorbent surface. In time, the concentration gradient is reduced owing to the adsorption of the dye molecules onto the vacant sites, leading to decreased adsorption during the later stages. As such, at higher concentrations, more Remazol Red RB molecules are left unadsorbed in the solution due to the saturation of binding sites resulting in decreased dye removal percentage. Under the same conditions, the adsorption capacity increases with increase in initial dye concentration. This is due to increasing concentration gradient which acts as increasing driving force to overcome all mass transfer resistances of the dye molecules between the aqueous and solid phase, leading to an increasing equilibrium sorption until sorbent saturation is achieved [23]. Moreover, the initial rate of adsorption was greater for higher initial dye concentration since the resistance to the dye uptake decreased as the mass transfer driving force increased.

3.2. Effect of temperature on adsorption process

The temperature has two major effects on the adsorption process. Increasing the temperature is known to increase the rate of diffusion of the adsorbate molecules across the external boundary layer and in the internal pores of the adsorbent particle, owing to the decrease in the viscosity of the solution. In addition, changing the temperature will change the equilibrium capacity of the adsorbent for a particular adsorbate [24]. The effect of temperature on the adsorption of Remazol Red RB onto modified clay sample is shown in Fig. 5. The results revealed that the adsorption capacity increased with increasing temperature from 298 to 313 K and to 333 K, showing that this process is endothermic. This kind of temperature dependence of the amount of the dye adsorbed may reflect the increase in the case with which the dye penetrates into the modified clay because of its larger

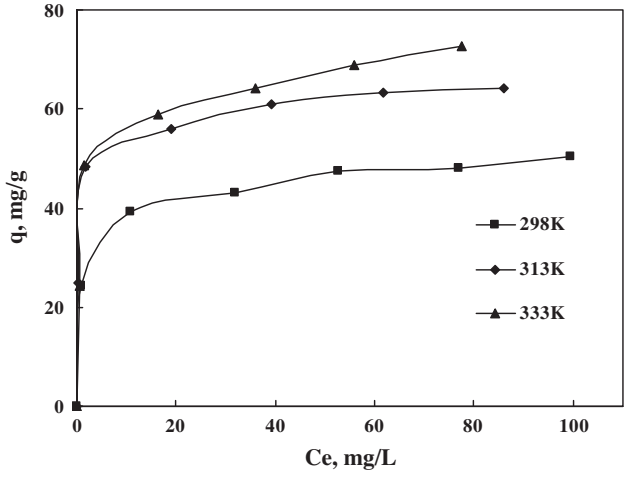

Fig. 5. The variation of the amount adsorbed (q) vs. equilibrium concentration (C_{eq}) at various temperatures. Contact time 90 min, stirring speed 90 min^{-1}, and pH natural.

diffusion coefficient. In fact, a possible mechanism of interaction is the reaction between positive-charged functional groups of the adsorbent and the anionic group in the dye molecules; such a reaction could be favored at higher temperatures [24]. In addition, as seen from Fig. 5, while a high adsorption efficiency was observed at low equilibrium concentrations, the adsorbed amount of dye remains almost constant after reaching surface saturation. The observed increase in adsorption efficiency for 150 mg/L when the adsorption was carried out at 333 K can be explained by the increased diffusion of dye molecules to the interlayer region with increasing temperature.

3.3. The effect of pH on the adsorption capacity, zeta potential, and conductivity

Fig. 6 shows the change in adsorption capacity and zeta potential values with initial pH values of initial Remazol Red RB concentration of 100 mg/L for 298 K. As shown in Fig. 6, the amount adsorbed increases with increasing pH up to neutral pH value and then decreases. It was also seen from this figure that zeta potential values of the particles have first sharply reduced and then slightly, with increased pH. After pH = 1, the sign of surface charge of particles change and negative values of zeta potential gradually decrease with increasing pH. The observed high negative value at low pH region and this change with pH could be based on the interaction both dye molecules and modified organo clay with suspension pH, because pH affects the ionization of dye molecules. Organoclay particles having a very high surface charge at natural pH (+74.4 mV) reaches the value of −55.4 mV as a result of adsorption of dye at the pH of 1. The changing of sign of the charge and a potential change of approximately 80 mV indicates the protonation of the SO_3 groups and pyridine groups of the azo structure at this pH. Depending on this, it can be said that the dye molecules are adsorbed on the clay surface as they are hydrophobic. It is understood that dye molecules is also connected to the clay surface through the electrostatic interactions with reduction in the degree of protonation and the reduction of negative values of zeta potentials of the particles in parallel with the increase in the amounts of adsorbed particles up to neutral pH value. The reduction of the amount adsorbed after this value is slightly going along with a reduction in the zeta potentials. This situation can be explained by hydroxyl ion adsorption onto clay surface, hydrophobic binding of dye molecules, and deprotonation of hydroxyl groups of dye molecules. Similar observation was obtained by Ada et al. [25] where the maximum adsorption capacity of reactive blue dye onto ZnO fine powder was obtained at pH 4. Jun Ma et al. [26] have studied the adsorption behavior of four anionic dyes—Methyl orange (MO), Orange IV (OIV), reactive brilliant red X-3B (X-3B), and Acid fuchsine (AF) – on ammonium-functionalized MCM-41 (NH_3^+-MCM-41) from aqueous medium and they found that at the pH range from 4.0 to 8.0, the adsorption capacity of the dye was slightly changed by pH. However, at pH above 8.0, the adsorption capacity of dye decreased significantly due to the increasing number of hydroxyl groups and the unstable structure of NH_3^+-MCM-41.

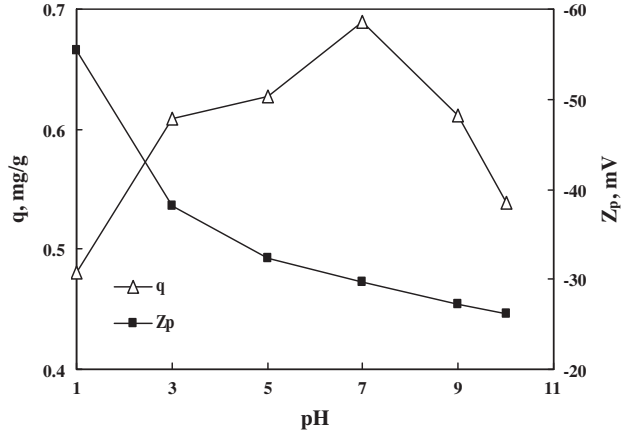

Fig. 6. The variation of both the amount adsorbed (q) and zeta potential with suspension pH.

The variation of conductivity and zeta potential values with initial pH values of initial Remazol Red RB concentration of 100 mg/L for 298 K are shown in Fig. 7. The observed decreases in conductivity values at pH 3 and 7 might be associated with reduction of protonization degree and the beginning of deprotonization (the loss of hydroxyl and proton), respectively.

3.4. Adsorption kinetics

The rate constant of adsorption is determined from the first-order rate expression given by Lagergren and Svenska [27]:

$$\ln(q_e - q_t) = \ln q_e - k_1 t \tag{3}$$

where q_e and q_t are the amounts of Remazol Red RB adsorbed (mg g^{-1}) at equilibrium and at time t (min), respectively, and k_1 is the rate constant of adsorption (s^{-1}). The obtained results in this study did not fit with the first-order model (Table 1). This shows that the adsorption of Remazol Red RB onto modified clay is not a first-order reaction. The second-order kinetic model is expressed as [28]:

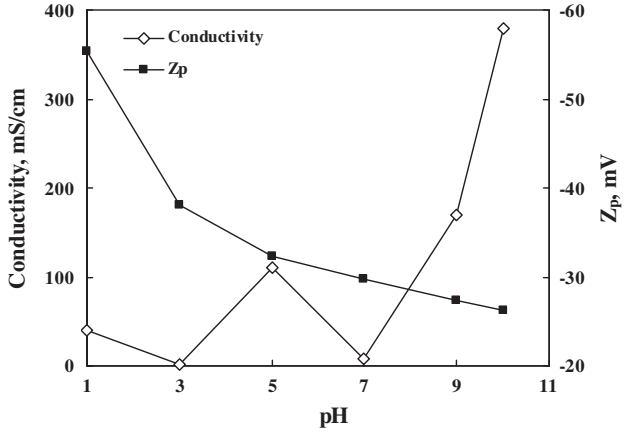

Fig. 7. The variation of both zeta potential and electrical-conductivity values with suspension pH.

$$t/q_t = 1/k_2 q_e^2 + t/q_e \quad (4)$$

where k_2 is the rate constant of second-order adsorption ($g\,mg^{-1}\,s^{-1}$). If the second-order kinetics is applicable, then the plot of t/q_t vs. t should show a linear relationship. There is no need to know any parameter beforehand and the equilibrium adsorption capacity, q_e, can be calculated from Eq. (4). Also, it is more likely to predict the behavior over the whole range of adsorption. Values of k_2 and q_e were calculated from the intercept and slope of the plots of t/q_t vs. t. The linear plots of t/q_t vs. t (Figs. 8–10) show a good agreement between experimental and calculated q_e values (Table 1). The correlation coefficients for the second-order kinetic model are greater than 0.999 indicating the applicability of this kinetic equation and the second-order nature of the adsorption process of Remazol Red RB on modified clay. Similar phenomena have been observed in the biosorption of Remazol black B on biomass [29] and adsorption of congo red [30] and 2-chlorophenol [31] on coir-pith carbon.

3.5. Mechanism of adsorption

The removal of Remazol Red RB by adsorption on modified clay was found to be rapid at the initial period of contact time and then to become constant with the increase in contact time. The mechanism for the removal of dye by adsorption may be assumed to involve the following four steps [32]:

- Migration of dye from the bulk of the solution to the surface of the adsorbent.
- Diffusion of dye through the boundary layer to the surface of the adsorbent.
- Adsorption of dye at an active site on the surface of adsorbent.
- Intra-particle diffusion of dye into the interior pores of the adsorbent particle.

The boundary layer resistance will be affected by the rate of adsorption and increase in contact time, which will reduce the resistance and increase the mobility of dye during adsorption. The uptake of dye at the active sites of adsorbent can mainly be governed by either liquid phase mass transfer rate or intra-particle mass transfer rate.

The adsorbate species are most probably transported from the bulk of the solution into the solid phase through intra-particle diffusion/transport process, which is often the rate limiting step in many adsorption processes. The possibility of intra-particle diffusion was explored by using the intra-particle diffusion model [33].

$$q_t = k_{dif} t^{1/2} + C \quad (5)$$

where C is the intercept and k_{dif} is the intra-particle diffusion rate constant ($mg\,s^{-1/2}\,g^{-1}$). The values of q_t were found to be linearly correlated with values of $t^{1/2}$. The k_{dif} values were calculated by using correlation analysis (Table 1). This functional relationship corresponds to the characteristic of intra-particle diffusion [34]. The intra-particle diffusion plots have been given in Figs. 11–13. The values of intercept (Table 1) give an idea about the boundary layer thickness, i.e. the larger the intercept, the greater is the boundary layer effect [35]. Such types of plots may present multilinearity, implying that two or more steps occur [36,37]. The sharper first-stage portion is the external surface adsorption stage. The second portion is the gradual adsorption stage, where the intra-particle diffusion is rate-limited. The third portion is the final equilibrium stage, where the intra-particle diffusion starts to slow down due to extremely low solute concentration in the solution. A good correlation of rate data in this model can justify the mechanism [38]. The applicability of intra-particle diffusion model indicates that it is the rate-determining step. As seen in Figs. 11–13, the plots are not linear over the whole time range, implying that more than one process affects the Remazol Red RB adsorption. The multiple natures of these plots can be explained in terms of a few processes, i.e. boundary-layer diffusion which gives the initial part of the plot and the intra-particle diffusion which gives further the two linear parts. If the intra-particle diffusion is the

Table 1
Kinetic values calculated for Remazol Red RB adsorption onto modified clay

Initial concentration (mg/L)	Temp. (K)	Pseudo-first-order	Pseudo-second-order				Intraparticle diffusion					
		R^2	k_2 ($g\,mg^{-1}\,s^{-1}$)	R^2	$q_{e,exp}$ (mg/g)	$q_{e,cal}$ (mg/g)	k_{i1} ($mg\,s^{-1/2}\,g^{-1}$)	R^2	C	k_{i2} ($mg\,s^{-1/2}\,g^{-1}$)	R^2	C
25	298	0.8179	97.261	0.9985	24.26	24.45	0.0498	0.9217	19.16	0.0336	0.3777	21.03
50	298	0.6299	224.710	0.9978	39.22	41.32	0.4425	0.8698	12.84	0.0446	0.9641	35.73
75	298	0.4599	285.927	0.9963	43.14	46.08	0.5835	0.8263	9.77	0.0452	0.8517	40.14
100	298	0.7080	328.828	0.9953	47.36	49.26	0.6649	0.8675	7.83	0.0320	0.5697	44.27
125	298	0.6679	405.890	0.9963	48.14	50.25	0.0066	0.7525	25.07	0.0347	0.6716	45.24
150	298	0.6588	477.594	0.9947	50.40	51.02	0.7074	0.7737	8.99	−0.0371	0.8424	52.94
25	313	0.1264	−197640	1.000	24.80	24.75	0.0032	0.8245	24.53	−0.0029	0.7100	25.03
50	313	0.7482	1021.408	0.999	48.24	48.54	0.2869	0.8543	30.41	−0.0222	0.3460	50.20
75	313	0.6780	998.318	0.999	55.88	58.14	0.3642	0.8731	33.34	0.0703	0.7694	50.49
100	313	0.8407	1529.850	0.999	60.90	61.73	0.4334	0.8328	33.98	0.0387	0.3454	57.23
125	313	0.5388	1712.030	0.999	63.22	65.36	0.4088	0.9692	38.73	0.0440	0.6442	60.28
150	313	0.6087	1709.220	0.999	64.08	67.11	0.5388	0.8634	33.53	0.0404	0.5340	61.81
25	333	0.0777	210.060	0.9998	24.33	24.81	0.0670	0.7027	20.51	0.0167	0.9499	23.06
50	333	0.4857	875.483	0.9994	48.64	49.50	0.2727	0.9901	31.72	0.0090	0.9791	47.99
75	333	0.6600	1502.500	0.9996	57.76	59.17	0.2246	0.7346	42.65	0.0224	0.9626	56.16
100	333	0.6550	1889.820	0.9993	61.04	62.50	0.2775	0.9659	43.28	0.0482	0.4398	57.35
125	333	0.6377	2510.790	0.9993	63.98	65.36	0.3377	0.8078	43.28	0.0401	0.2994	60.78
150	333	0.6741	3477.940	0.9991	72.58	72.46	0.2805	0.9584	52.27	−0.0520	0.7793	76.70

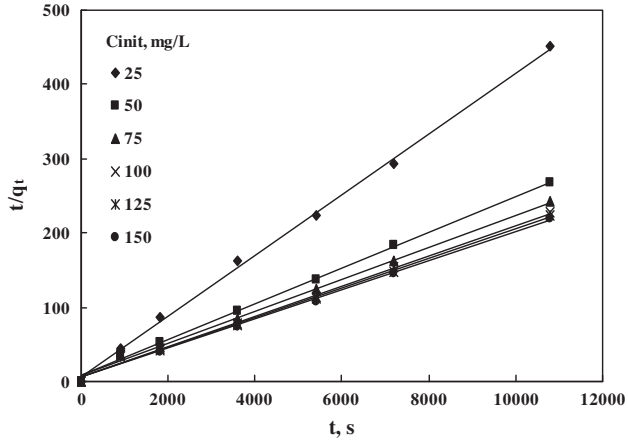

Fig. 8. Plot of t/q_t vs. time at different initial concentrations for 298 K.

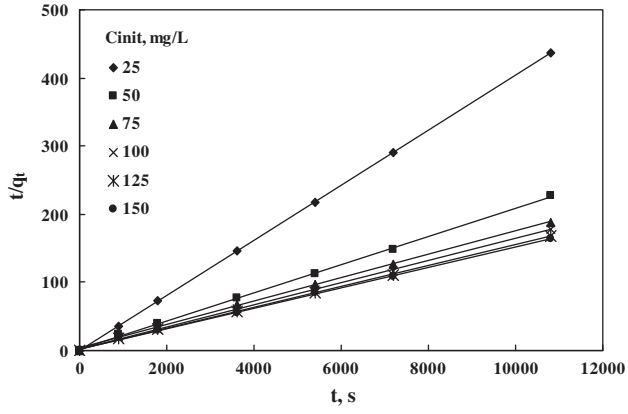

Fig. 9. Plot of t/q_t vs. time at different initial concentrations for 313 K.

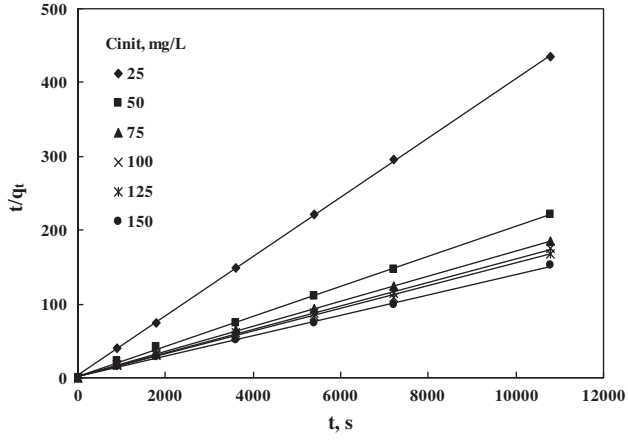

Fig. 10. Plot of t/q_t vs. time at different initial concentrations for 333 K.

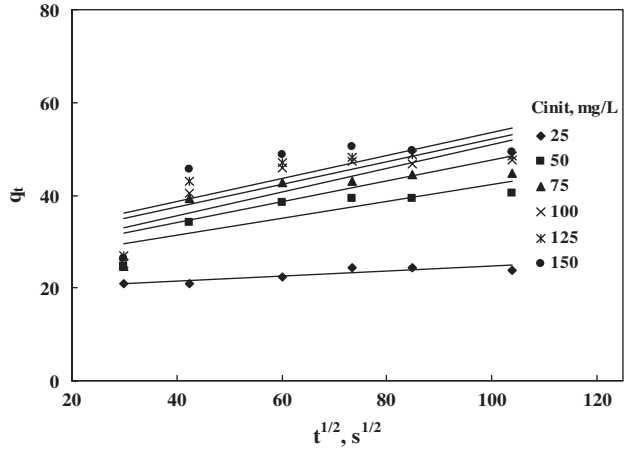

Fig. 11. Plot of q_t vs. $t^{1/2}$ at different initial concentrations for 298 K.

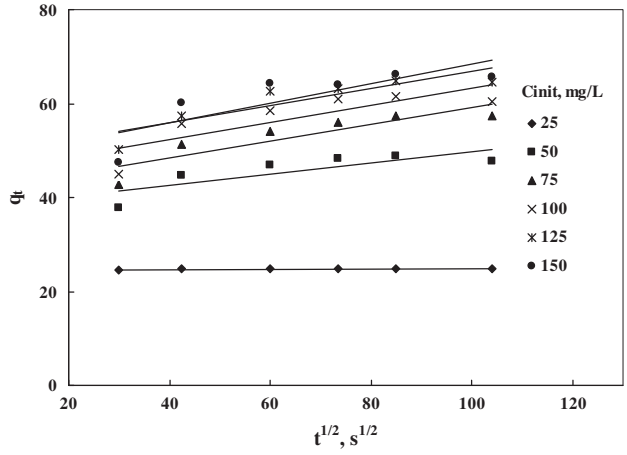

Fig. 12. Plot of q_t vs. $t^{1/2}$ at different initial concentrations for 313 K.

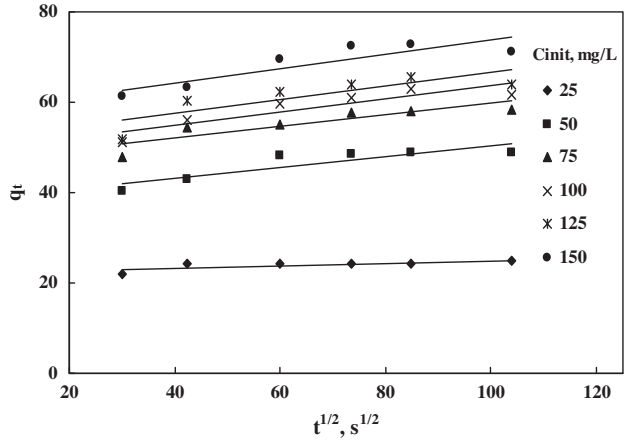

Fig. 13. Plot of q_t vs. $t^{1/2}$ at different initial concentrations for 333 K.

only rate-controlling step, then the plot passes through the origin, if not, the boundary-layer diffusion affects the adsorption to some extent [39]. From Figs. 11–13, the linear portions of the plots for a wide range of contact time between adsorbent and adsorbate do not pass through the origin. This deviation from the origin or near saturation may perhaps be due to the difference in the rate of mass transfer in the initial and final stages of adsorption. Further, such deviation from origin indicates that the pore diffusion is not the only rate-controlling step [28,33]. As seen from Table 1, the regression coefficients for external and internal diffusion are quite small. Only, internal diffusion coefficients are higher for low concentrations at 333 K. As a result, pseudo-second-order kinetic models are applicable for Remazol Red RB adsorption on modified clay. Table 1 also indicates that the regression coefficients for the linear plots from the pseudo-second-order equation are greater than that of the intra-particle diffusion.

From the pseudo-second-order rate constant k_2 (Table 1), the activation energy E_a for adsorption of Remazol Red RB on modified clay was determined using the Arrhenius equation (Eq. (6)). By plotting $\ln k_2$ vs. $1/T$, E_a was obtained from the slope of the linear plot (figure not shown).

$$\ln k = \ln A - E_a/RT \tag{6}$$

where E_a is activation energy ($J\,mol^{-1}$); R is the gas constant ($8.314\,J\,mol^{-1}\,K^{-1}$), and T is the adsorption temperature (K). The results obtained are $34.49\,kJ\,mol^{-1}$ and $40.27\,kJ\,mol^{-1}$ for initial dye concentrations of 75 and 150 mg/L, respectively. The magnitude of activation energy gives an idea about the type of adsorption which is mainly physical or chemical. E_a for physisorption is usually $<40\,kJ\,mol^{-1}$, whereas it is higher in the case of chemisorption [23]. According to literature, the adsorption process of Remazol Red RB onto modified clay may be physical adsorption [40]. This claims that the uptake rate of the basic dye on modified clay could be described by a pseudo-second-order rate expression based on the strong electrostatic interactions between the adsorbent and the dye.

3.6. Adsorption isotherms

In order to determine the mechanism of Remazol Red RB adsorption on the modified clay sample at 298, 313, and 333 K, the experimental data were applied to the Langmuir, BET, Freundlich, Temkin, D–R, Halsey, Harkins–Jura, Smith, and Henderson isotherm equations. The constant parameters of the equations for this system were calculated by regression using the linear form of the isotherm equations and SPSS 10.0 software. The results are given in Table 2, together with the isotherm equations. Figs. 14–17 show the isotherms belonging to Langmuir, Freundlich, Temkin and D–R adsorption models of Remazol Red RB on the modified clay at 298, 313, and 333 K temperatures, respectively.

The Langmuir isotherm theory assumes monolayer coverage of adsorbate over a homogeneous adsorbent surface, i.e. the surface consists of identical sites, equally available for adsorption and with equal energies of adsorption. Therefore, at equilibrium, a saturation point is reached where no further adsorption can occur. Adsorption is assumed to take place at specific homogeneous sites with the adsorbent and once a dye molecule occupies a site, no further adsorption can take place at the site and there is no significant interaction among the adsorbed species [41]. Fig. 14 shows the Langmuir isotherms for Remazol Red RB adsorption at different temperatures. From the correlation coefficient (R^2) values that are regarded as a measure of the goodness-of-fit of experimental data on the isotherm's model (Table 2), it was elucidated that the Langmuir equation represents the Remazol red adsorption process on the modified clay at the different solution temperatures very well; the R^2 values were all higher than 0.99, indicating a very good mathematical fit. This fitting also suggests that the adsorption of Remazol Red RB occurs predominantly through effective electrostatic interactions. On the other hand, from Table 2, it may be predicted that the dye adsorption on the organoclay is an endothermic process, where the monolayer adsorption capacity of dye (q_m) increased as solution temperature was increased. Among K values calculated from the Langmuir isotherm model, as can be seen from Table 2, the highest value is obtained for 333 K. A higher value of K implies strong interactions between dye molecules and modified clay.

The essential characteristic of the Langmuir isotherm can be expressed by the dimensionless constant called equilibrium parameter, R_L, defined by

$$R_L = 1/(1 + KC_0) \tag{7}$$

where K is the Langmuir constant and C_0 is the highest initial dye concentration, R_L values indicate the type of isotherm to be irreversible ($R_L = 0$), favorable ($0 < R_L < 1$), linear ($R_L = 1$) or unfavorable ($R_L > 1$). The R_L values for the adsorption of Remazol Red RB dye on the modified clay sample were calculated. The values of R_L in the present study were found to be 1.46×10^{-4} at 298 K, 0.0065 at 313 K, and 0.0066 at

Table 2
Applicability of isotherm equations to Remazol Red RB adsorption data of modified clay/dye system at different temperatures and their constant parameters

Isotherm	Equation	Parameters	298 K	313 K	333 K
Langmuir	$C/q = 1/kq_m + (1/q_m)C$	q_m	0.502	1.01	69.93
		k	45.65	64.1	1.524
		R^2	0.9972	0.9999	0.9903
Freundlich	$\ln q = \ln k + n \ln C$	n	0.1473	0.1439	0.1701
		k	0.5130	35.94	3.5260
		R^2	0.9854	0.8943	0.7761
BET	$C/q(1-C) = 1/(q_m k) + [(k-1/q_m k)]C$	q_m	–	–	–
		k	–	–	–
		R^2	0.4906	0.7675	0.8948
Dubinin–Radukevisch	$\ln q = K\varepsilon^2 + \ln q_{D-R}$	K	-5×10^{-9}	-2×10^{-7}	-4×10^{-9}
		$q_{D\text{-}R}$	0.4820	61.01	0.689
		R^2	0.9885	0.8019	0.8320
		E (kJ/mol)	10.0	1.581	11.18
Halsey	$\ln q = (1/n)\ln k - (1/n)\ln[\ln(1/C)]$	n	–	–	–
		k	–	–	–
		R^2	0.4450	0.6007	0.6428
Harkins–Jura	$1/q^2 = (B/A) - (1/A)\log C$	B	–	–	–
		A	–	–	–
		R^2	0.9844	0.7755	0.6112
Smith	$q = W_b - W\ln(1-C)$	W	–	–	–
		W_b	–	–	–
		R^2	0.5693	0.4200	0.6068
Henderson	$\ln[-\ln(1-C)] = \ln k + n \ln q$	n	–	–	–
		k	–	–	–
		R^2	0.9163	0.8650	0.7650
Temkin	$q_e = (RT/b_T)\ln a_T + (RT/b_T)\ln C_e$	b_T	47372.3	42730.4	36332.83
		a_T	14435.4	55609.5	11015.81
		R^2	0.9948	0.9483	0.8505

q, adsorption capacity of Remazol Red RB (mg/g); q_m, monolayer adsorption capacity; C, equilibrium concentration; n, k, K, A, B, W_a and W are constant parameters for the isotherm equations.

333 K indicating that the adsorption of Remazol Red RB on organo clay is favorable [42]. The experimental dye uptake values obtained have also been analyzed using Freundlich equation. In Freundlich adsorption isotherm, the model assumes a heterogeneous surface with a nonuniform distribution of heat of adsorption over the surface. From Table 2, the high R^2 value was observed for 298 K, but it was low for 313 K and 333 K.

A comparison of the isotherm constants along with regression coefficients (R^2) is presented in Table 2. Comparing the regression coefficient values for both the Langmuir and Freundlich isotherms, it was demonstrated that the Langmuir isotherm was the most appropriate isotherm to describe the equilibrium data for dye adsorption at the two studied temperatures.

The Temkin isotherm equation assumes that the heat of adsorption of all the molecules in the layer decreases linearly with coverage due to adsorbent–adsorbate interactions, and that the adsorption is characterized by a uniform distribution of the binding energies, up to some maximum binding energy Also,

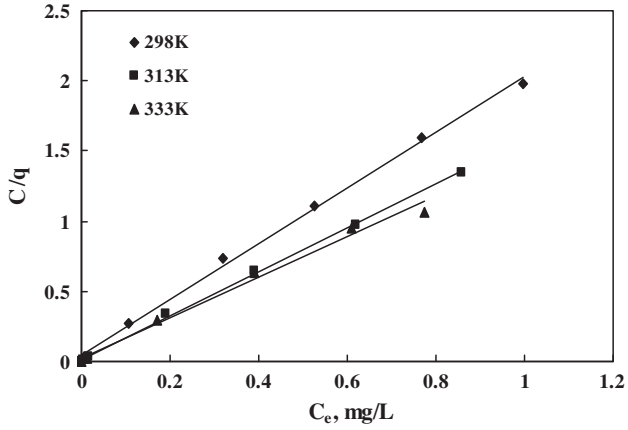

Fig. 14. Langmuir adsorption isotherms for Remazol Red RB adsorption at different temperatures.

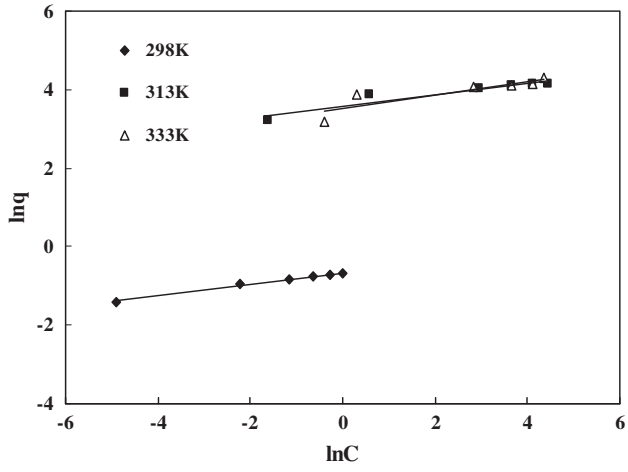

Fig. 15. Freundlich adsorption isotherms for Remazol Red RB adsorption at different temperatures.

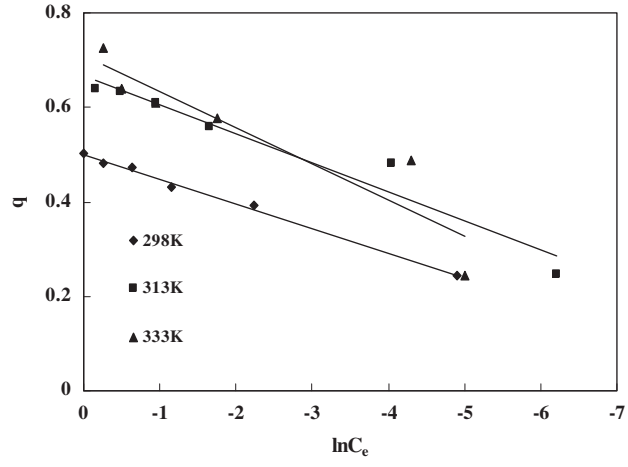

Fig. 16. Temkin adsorption isotherms for Remazol Red RB adsorption at different temperatures.

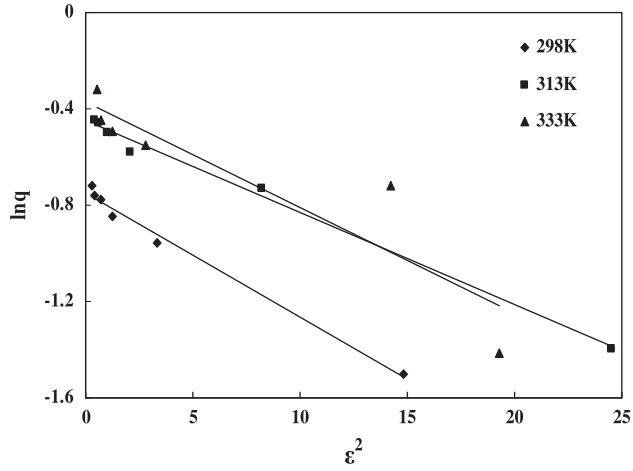

Fig. 17. Dubinin–Radukevisch adsorption isotherms for Remazol Red RB adsorption at different temperatures.

the Temkin equation suggests a linear decrease of sorption energy as the degree of completion of the sorptional centers of an adsorbent is increased [40,42,43]. The Temkin isotherm equation is given as follows,

$$q_e = (RT/b_T)\ln a_T + (RT/b_T)\ln C_e \quad (8)$$

where b_T and a_T are constants related to the heat of adsorption and equilibrium binding constant corresponding to the maximum binding energy, respectively. A plot of q_e vs. $\ln C_e$ enables the determination of the isotherm constants a_T and b_T (Fig. 16). The obtained values for a_T and b_T are tabulated together with the value of the correlation coefficient in Table 2. The correlation coefficients calculated suggest that the Temkin isotherm represents the equilibrium data very well for 298 K. This reveals that the dye adsorption at 298 K is characterized by a uniform distribution of binding energies up to some maximum binding energy [44]. The increase in temperature probably leads to the decreasing uniformity.

The D–R model was used to determine the characteristic porosity and the apparent free energy of adsorption. D–R isotherm equation [33,43,45].

$$\ln q_e = K\varepsilon^2 + \ln q_{\mathrm{D-R}} \quad (9)$$

where q_e is the amount adsorbed of dye at equilibrium concentration (mg/g); $q_{\mathrm{D-R}}$ is D–R maximum adsorption capacity of the dye (mg/g), K is the D–R constant (the porosity factor, $\mathrm{mol^2\,J^{-2}}$), and ε is the Polanyi potential given by the equation below [40–43]:

$$\varepsilon = RT\ln(1 + 1/C_e) \quad (10)$$

where C_e is the equilibrium concentration of the dye (mg/L), R is the gas constant (8.314 J K^{-1} mol^{-1}, and T is the temperature (K). The D–R constant (K) can give valuable information about the mean energy of adsorption by using Eq. (11) [40–42,45].

$$E = (-2K)^{-1/2} \quad (11)$$

where E is the mean adsorption energy. The results were shown in Table 2. In addition, the mean adsorption energy (E) from the D–R isotherm, defined as the free energy change when one mole of ion is transferred from infinity in solution to the surface of the solid, could be used to estimate the type of adsorption. The adsorption behavior could be predicted as the physical adsorption in the range of 1–8 kJ/mol and the chemical adsorption in more than 8 kJ/mol [40–42,45]. The E values (Table 2) of 10.0, 1.581, and 11.18 kJ/mol for the adsorption of Remazol Red RB at 298 K, 313 K, and 333 K, respectively indicated that the adsorption of dye onto the modified clay occurs via strong electrostatic interactions.

3.7. Adsorption thermodynamics

Thermodynamic quantities for the adsorption of Remazol Red RB onto organo clay surface have been determined by considering the specific amounts of surfactant adsorbed. These are isosteric adsorption enthalpy $(\Delta H_{ads})_q$ and isosteric adsorption entropy $(\Delta S_{ads})_q$, which were statistically calculated by using least squares method and experimental data. These quantities were calculated using Eqs. (12) and (13) [46]. In these calculations, the amounts of the dye adsorbed at the different temperatures correspond to the different equilibrium adsorbate concentrations in which adsorption capacity values exhibit the tendency to be constant. The results are given in Table 3.

$$d(\ln C)/d(1/T) = (\Delta H_{ads})/R \quad (12)$$

$$d(\ln C)/d(\ln T) = (\Delta S_{ads})/R \quad (13)$$

where C and T in these equations represent the equilibrium dye concentration and absolute temperature, respectively.

$$\Delta G^o = -RT\ln K \quad (14)$$

where K (L/mg) is Langmuir isotherm constant, R is the gas constant (8.314 J K^{-1} mol^{-1}), and T is the temperature (K).

From experimental adsorption isotherms for Remazol Red RB adsorption on modified clay at different temperatures, the isosteric enthalpy of adsorption, ΔH_{ads}, can be determined by using Eq. (12) and the isosteric entropy of adsorption, ΔS_{ads}, can also be determined by using the Eq. (13). As can be seen from Table 3, the equilibrium concentrations used in the calculation of ΔH_{ads} and ΔS_{ads} are not values corresponding to the monolayer surface cover, but in these equilibrium concentrations, the values of adsorption capacity of the organo clay begin to be constant. From Table 3, it can be seen that the signs of ΔH_{ads} and ΔS_{ads} for adsorption of Remazol Red RB onto modified clay are positive and negative, respectively. As temperature is increased, the amount of dye adsorbed is increased, implying the endothermic nature of the adsorption process. This increase also verifies the positive sign expected of $(\Delta H_{ads})_q$. The negative values of entropy change, ΔS states a decreased disorder at the solid–liquid interface during dye sorption. As the temperature is increased, the mobility of dye ions increases causing the ions to escape from the solid phase to the liquid phase. Therefore, the amount of dyes adsorbed will decrease, whereas the negative values of ΔG^o indicated the spontaneous and feasible nature of the adsorption process at the range of temperatures and the different dye concentrations. As

Table 3
Amounts adsorbed and equilibrium concentration values for the 298, 313, and 333 K temperatures and the thermodynamic quantities for modified clay/dye system

Parameters	Temperature (K)		
	298	313	333
Equilibrium concentration, C^a (mg/L)	0.74	0.67	0.20
Adsorption capaciy, q (mg/g)	0.242	0.243	0.248
Isosteric adsorption enthalpy, $(\Delta H_{ads})_q$ (kJ mol^{-1})	31.03		
Isosteric adsorption entropy, $(\Delta S_{ads})_q$ (kJ mol^{-1} K^{-1})	−0.1		
Free energy of specific adsorption, $(\Delta G_{ads})_q$ (kJ mol^{-1})	−9.466	−10.826	−1.166

[a]The values in which adsorption capacity of the organo clay particles is constant.

a result, it can be said that the adsorption results obtained from modified clay/aqueous dye solution system will shed light on adsorption processes in which similar adsorbents and adsorbates are used.

4. Conclusion

In this study, the adsorption of Remazol Red RB onto modified clay sample was investigated at 298, 313, and 333 K. The adsorption studies were carried out as a function of contact time, initial dye concentration, solution pH, and temperature. Percentage removal of the dye molecule decreased with increase in initial dye concentration, while it increased with increase in contact time. Equilibrium adsorption was achieved in about 90 min. The adsorption is dependent on concentration, pH, and temperature of the solution. Solution pH affects the surface charge of the adsorbent and the degree of ionization of adsorbate. Experimental equilibrium data provided best fit with the Langmuir isotherm model, indicating monolayer sorption on a homogenous surface. The monolayer sorption capacity increased with increase in temperature from 298 K to 313 K and 333 K. Adsorption of Remazol Red RB on modified clay sample seems to be a favored process. The correlation coefficients calculated from Temkin isotherm equation (Table 2) reveals that the dye adsorption at 298 K is characterized by a uniform distribution of binding energies up to some maximum binding energy. The increasing temperature probably leads to a decrease of uniformity. According to D–R isotherm model, adsorption of Remazol Red RB onto the modified clay occurs via strong electrostatic interactions. The calculated Ea values by using the Arrhenius equation implies that the adsorption of Remazol Red RB on modified clay is physically controlled, which involved strong electrostatic interactions between adsorbent and dye. Thermodynamic parameters such as change in Gibbs free energy ΔG^{o}, isosteric adsorption enthalpy $(\Delta H_{ads})_q$, and isosteric adsorption entropy $(\Delta S_{ads})_q$ were also estimated. Thermodynamic analysis suggests that adsorption of Remazol Red RB by organo clay was a spontaneous and endothermic process. According to the present findings, it can be said that the adsorption results obtained from modified clay/aqueous dye solution system will shed light on adsorption processes in which similar adsorbents and adsorbates are used.

References

[1] E. Chibowski, A.O. Ortega, M. Espinosa-Jiménez, R. Perea-Carpio, L. Holysz, Study of the leacril dyeing process by a cationic dye from an emulsion system, J. Colloid Interface Sci. 235 (2001) 283–288.
[2] J.J. Gooding, R.G. Compton, C.M. Brennan, J.H. Atherton, The dyeing of nylon and cotton cloth with azo dyes: kinetics and mechanism, J. Colloid Interface Sci. 180 (1996) 605–613.
[3] L.R. Bergsten-Torralba, M.M. Nishikawa, D.F. Baptista, D.P. Magalhães, M. da Silva, Decolorization of different textile dyes by *Penicillium simplicissimum* and toxicity evaluation after fungal treatment, Braz. J. Microbiol. 40 (2009) 808–817.
[4] S. Chowdhury, R. Mishra, P. Saha, P. Kushwaha, Adsorption thermodynamics, kinetics and isosteric heat of adsorption of malachite green onto chemically modified rice husk, Desalination 265 (2011) 159–168.
[5] S. Chowdhury, P. Saha, Sea shell powder as a new adsorbent to remove Basic Green 4 (Malachite Green) from aqueous solutions: equilibrium, kinetic and thermodynamic studies, Chem. Eng. J. 164 (2010) 168–177.
[6] P. Saha, S. Chowdhury, S. Gupta, I. Kumar, Insight into adsorption equilibrium, kinetics and thermodynamics of Malachite Green onto clayey soil of Indian origin, Chem. Eng. J. 165 (2010) 874–882.
[7] Papita Das Saha, Shamik Chowdhury, Madhurima Mondal, Keka Sinha, Biosorption of Direct Red 28 (Congo Red) from aqueous solutions by eggshells: batch and column studies, Sep. Sci. Technol. 47 (2012) 12–123.
[8] A. Szyguła, E. Guibal, M.A. Palacín, M. Ruiz, A.M. Sastre, Removal of an anionic dye (Acid Blue 92) by coagulation–flocculation using chitosan, J. Environ. Manage. 90 (2009) 2979–2986.
[9] A.N. Fernandes, C.A.P. Almeida, C.T.B. Menezes, N.A. Debacher, M.M.D. Sierra, Removal of methylene blue from aqueous solution by peat, J. Hazard. Mater. 144 (2007) 412–419.
[10] V. Dulman, S.M. Cucu-Man, Sorption of some textile dyes by beech wood sawdust, J. Hazard. Mater. 162 (2009) 1457–1464.
[11] S.W. Won, G. Wu, H. Ma, Q. Liu, Y. Yan, L. Cui, C. Liu, Yeoung-Sang Yun, Adsorption performance and mechanism in binding of Reactive Red 4 by coke waste, J. Hazard. Mater. 138 (2006) 370–377.
[12] S. Wang, Y. Boyjoo, A. Choueib, Z.H. Zhu, Removal of dyes from aqueous solution using fly ash and redmud, Water Res. 39 (2005) 129–138.
[13] I.D. Mall, V.C. Srivastava, N.K. Agarwal, Removal of Orange-G and Methyl Violet dyes by adsorption onto bagasse fly ash—kinetic study and equilibrium isotherm analyses, Dyes Pigm. 69 (2006) 210–223.
[14] A. Gil, F.C.C. Assis, S. Albeniz, S.A. Korili, Removal of dyes from wastewaters by adsorption on pillared clays, Chem. Eng. J. 168 (2011) 1032–1040.
[15] W.T. Tsai, C.Y. Chang, C.H. Ing, C.F. Chang, Adsorption of acid dyes from aqueous solution on activated bleaching earth, J. Colloid Interface Sci. 275 (2004) 72–78.
[16] A. Gürses, S. Karaca, Ç. Doğar, R. Bayrak, M. Açıkyıldız, M. Yalçın, Determination of adsorptive properties of clay/water system: methylene blue sorption, J. Colloid Interface Sci. 269 (2004) 310–314.
[17] S. Yariv, H. Cross, Organo-Clay Complexes and Interaction, Marcel Dekker, New York, 2002.
[18] A. Tabak, E. Eren, B. Afsin, B. Çağlar, Determination of adsorptive properties of a Turkish sepiolite for removal of reactive blue 15 anionic dye from aqueous solutions, J. Hazard. Mater. 161 (2009) 1087–1094.
[19] A.S. Tunali, R. Uysal, Untreated clay with high adsorption capacity for effective removal of C.I. Acid red 88 from aqueous solutions: batch and dynamic flow mode studies, Chem. Eng. J. 162 (2010) 591–598.
[20] V. Vimonses, S. Lei, B. Jin, C.W.K. Chow, C. Saint, Kinetic study and equilibrium isotherm analysis of Congo red adsorption by clay material, Chem. Eng. J. 148 (2009) 354–364.
[21] M.H. Karaoğlu, M. Doğan, M. Alkan, Kinetic analysis of reactive blue 22 adsorption on kaolinite, Desalination 256 (2010) 154–165.
[22] Y. Xubiao, W. Chaohai, K. Lin, H. Yun, X. Xiaoqi, W. Haizhen, Developments of organovermiculite-based adsorbent for removing anionic dye from aqueous solution, J. Hazard. Mater. 180 (2010) 499–507.

[23] S. Chowdhury, S. Chakraborty, P. Saha, Biosorption of Basic Green 4 from aqueous solution by *Ananas comosus* (pineapple) leaf powder, Colloids Surf, B 84 (2011) 520–527.
[24] M. Espinosa-Jiménez, R. Padilla-Weigand, A. Ontiversos-Ortega, R. Perea-Carpio, Thermodynamic characterization of the adsorption process of mordant black 17 dye onto polyamide fabric, Macromol. Mater. Eng. 286 (2001) 302–308.
[25] K. Ada, A. Ergene, S. Tan, E. Yalc, Adsorption of Remazol Brilliant Blue R using ZnO fine powder: equilibrium, kinetic and thermodynamic modeling studies, J. Hazard. Mater. 165 (2009) 637–644.
[26] Q. Qin, J. Ma, K. Liu, Adsorption of anionic dyes on ammonium-functionalized MCM-41, J. Hazard. Mater. 162 (2009) 133–139.
[27] Lagergren, B.K. Svenska, Zur theorie der sogenannten adsorption geloester stoffe, Veternskapsakad Handlingar 24 (1898) 1–39.
[28] A.R. Nesic, S.J. Velickovic, D.G. Antonovic, Characterization of chitosan/montmorillonite membranes as adsorbents for Bezactiv Orange V-3R dye, J. Hazard. Mater. 209–210 (2012) 256–263.
[29] Z. Aksu, S. Tezer, Equilibrium and kinetic modeling of biosorption of Remazol Black B by *Rhizopus arrhizus* in a batch system: effect of temperature, Process Biochem. 36 (2000) 431–439.
[30] C. Namasivayam, D. Kavitha, Removal of Congo Red from water by adsorption onto activated carbon prepared from coir pith, an agricultural solid waste, Dyes Pigm. 54 (2002) 47–48.
[31] C. Namasivayam, D. Kavitha, Adsorptive removal of 2-chlorophenol by low-cost coir pith carbon, J. Hazard. Mater. B98 (2003) 257–274.
[32] Y. El Mouzdahir, A. Elmchaouri, R. Mahboub, A. El Anssari, A. Gil, S.A. Korili, M.A. Vicente, Interaction of stevensite with Cd^{2+} and Pb^{2+} in aqueous dispersions, Appl. Clay Sci. 35 (2007) 47–58.
[33] M. Doğan, M. Alkan, A. Türkyılmaz, Y. Özdemir, Kinetics and mechanism of removal of methylene blue by adsorption onto perlite, J. Hazard. Mater. B109 (2004) 141–148.
[34] K. Banerjee, P.N. Cheremisinoff, S.L. Cheng, Adsorption kinetics of o-xylene by fly ash, Water Res. 31 (1997) 249–261.
[35] S. Karaca, A. Gürses, M. Ejder, M. Açıkyıldız, Kinetic modeling of liquid-phase adsorption of phosphate on dolomite, J. Colloid Interface Sci. 277 (2004) 257–263.
[36] M. Doğan, Y. Özdemir, M. Alkan, Adsorption kinetics and mechanism of cationic methyl violet and methylene blue dyes onto sepiolite, Dyes Pigm. 75 (2007) 701–713.
[37] W.H. Cheung, Y.S. Szeto, G. McKay, Intraparticle diffusion processes during acid dye adsorption onto chitosan, Bioresour. Technol. 98 (2007) 2897–2904.
[38] N. Kamal Amin, Removal of reactive dye from aqueous solutions by adsorption onto activated carbons prepared from sugarcane bagasse pith, Desalination 223 (2008) 152–161.
[39] M. Uğurlu, A. Gürses, M. Açıkyıldız, Comparison of textile dyeing effluent adsorption on commercial activated carbon and activated carbon prepared from olive stone by $ZnCl_2$ activation, Micropor. Mesopor. Mater. 111 (2008) 228–235.
[40] A.H. Chen, Y.Y. Huang, Adsorption of Remazol Black 5 from aqueous solution by the templated crosslinked-chitosans, J. Hazard. Mater. 177 (2010) 668–675.
[41] M.A. Ahmad, N.K. Rahman, Equilibrium, kinetics and thermodynamic of Remazol Brilliant Orange 3R dye adsorption on coffee husk-based activated carbon, Chem. Eng. J. 170 (2011) 154–161.
[42] M.F. Elkady, A.M. İbrahim, M.M. Abd El-Latif, Assessment of the adsorption kinetics, equilibrium and thermodynamic for the potential removal of reactive red dye using eggshell biocomposite beads, Desalination 278 (2011) 412–423.
[43] P. Sivakumar, P.N. Palanisamy, Adsorption studies of Basic Red 29 by a nonconventional activated carbon prepared from Euphorbia antiquoruml, Int. J. Chem. Tech. Res. 1 (2009) 502–510.
[44] M.J. Temkin, V. Pyzhev, Recent modifications to Langmuir isotherms, Acta Physiochim. URSS 12 (1940) 217–222.
[45] L. Zhou, J. Jin, Z. Liu, X. Liang, C. Shang, Adsorption of acid dyes from aqueous solutions by the ethylenediamine-modified magnetic chitosan nanoparticles, J. Hazard. Mater. 185 (2011) 1045–1052.
[46] A. Gürses, M. Yalçın, M. Sözbilir, Ç. Doğar, The investigation of adsorption thermodynamics and mechanism of a cationic surfactant, CTAB, onto powdered active carbon, Fuel Process Technol. 81 (2003) 57–66.